GENERAL MOTORS CORPORATION

FINAL TECHNICAL REPORT

EXPERIMENTAL RESEARCH ON THE ELECTRIC VACUUM GYRO

Submitted to
National Aeronautics and Space Administration
Electronics Research Center
Cambridge, Massachusetts

Under Contract
No. NAS12-28

GM DEFENSE RESEARCH LABORATORIES

SANTA BARBARA, CALIFORNIA

PHYSICAL SCIENCES DEPARTMENT

TR66-52

OCTOBER 1966

Copy No 14

GENERAL MOTORS CORPORATION

FINAL TECHNICAL REPORT

EXPERIMENTAL RESEARCH ON THE ELECTRIC VACUUM GYRO

Submitted to
National Aeronautics and Space Administration
Electronics Research Center
Cambridge, Massachusetts

Under Contract
No. NAS12-28

GM DEFENSE RESEARCH LABORATORIES

SANTA BARBARA, CALIFORNIA

PHYSICAL SCIENCES DEPARTMENT

TR66-52

OCTOBER 1966

CONTENTS

ILLUSTRATIONS

SUMMARY

Development of electronic circuitry for suspending an electric vacuum gyro (EVG) rotor in the center of its electrode sphere is described. The suspension differs from previous circuitry in that the currents that develop the varying forces required to keep the rotor centered under acceleration loading are supplied by varying the phase between two constant currents rather than summing a constant and a variable current. This "phase modulation" approach has many important advantages over the "amplitude modulation" approach and its feasibility has been completely demonstrated.

The circuit features are discussed in detail, with complete schematics and suspension adjustment procedures included.

The system was completely checked out on the bench and then subjected to centrifuge tests and a strap-down drift test. The centrifuge tests show that the suspension has a g capability varying from 1.0g to 10.3g for a voltage excitation of 7.0 vdc to 21.0 vdc, respectively. Power consumption for the same range of voltage varied from 1.5 watts to 17.0 watts. The strap-down drift test demonstrated performance of the suspension with the gyro in operation, but, due to the poor mechanical quality of the gyro used, no verification of improved drift performance was possible.

Recommendations for future improvements are given.

SECTION I
INTRODUCTION

This report presents the results of experimental research on the electric vacuum gyro (EVG) sponsored by NASA under Contract NAS 12-28.

The electric vacuum gyro utilizes a rotor suspended free of all material contact—solid, liquid, or gaseous—by housing the rotor in high vacuum and supporting it with servo-controlled electric fields.

In practice, the rotor is spun about its principal axis of greatest inertia at very high angular rates. This spin axis then serves as an accurate stable directional reference in space which can be used in navigation systems, or as a vehicle attitude reference.

The quality of the directional reference is affected by the magnitude of disturbing torques on the gyro rotor. Potential sources of disturbing torques in the electric vacuum gyro, which can result in spin axis drift, are torques due to residual gas in the case, magnetic fields, and the electric suspending fields. Gas pressure in the vacuum envelope is maintained reliably at very low levels so that torques due to residual gas are negligible. Magnetic shielding around the gyro attenuates magnetic fields (10 gauss or less) to a level where magnetically induced torques are no problem; this leaves the electric suspending fields as the only significant source of error torque.

These torques arise in an indirect way since the suspending fields themselves produce only a negligible tangential component at the rotor surface (the field vector departs from the normal by only 10^{-13} radians). This implies then, that if the rotor was perfectly spherical and had its center of mass located at the center of figure of the sphere, there would be absolutely no torques present. In practice, however, it is not possible to make a perfect rotor, so that some departure from sphericity will always be present. In fact, a rotor which is spherical

at rest (which represents the easiest fabrication problem), will deform when turning because of centrifugal distortion. This asphericity, plus manufacturing tolerances, create problems related to rotor fabrication and rotor suspension design.

The minimizing of precession torques attributable to the suspension system can be translated into two practical electronic requirements: at low frequencies, say below 20 cps, the rotor positioning error with respect to the electrode sphere should be very small; secondly, the sum of the two mean square currents (directly related to the sum of the two forces) into diametrically opposite electrodes should vary as little as possible among electrode pairs. Rotor positioning errors result in a shifting of the center of buoyancy of the rotor from its center of figure and produce torques similar to those caused by rotor mass unbalance. Torques attributable to nonequality of the sums of forces from diametrically opposite electrodes arise because, with a nonspherical rotor (centrifugally distorted), the forces from opposite electrodes do not have the same line of action. Thus, each pair of electrodes produces a torque, and it can be shown that the prerequisite for zero resultant torque from all electrodes is that the sum of forces from all electrode pairs be equal.

In a suspension circuit previously developed at GM DRL, the magnitudes of forces on the rotor are varied by summing a variable magnitude current with a constant magnitude current. Circuits for maintaining constancy of sum of forces and low frequency centering are included, but are essentially add-on features which are difficult to integrate with the rest of the circuitry. The sum of forces circuitry requires use of nonlinear elements which are difficult to match and have questionable stability.

Based on experience acquired in working with this suspension, a concept was evolved for developing a new rotor suspension system that is simple and requires less power than the suspension presently in use (especially for space applications where the unit is exposed to low accelerations for most of its mission). This system would permit holding the sum of forces over pairs of electrodes constant to a much higher degree than is now possible, and also would maintain rotor

centering more accurately. Forces on the rotor are varied by changing the phase between two constant currents instead of summing a constant current and a variable current. The amplitude-modulated system and the phase-modulated system are compared in Figure 1 and, as can be seen, the conditions for sum of forces constancy are satisfied more naturally and simply with the phase-modulated system.

The program for developing a phase-modulated suspension was funded by NASA and is the subject of this report. Section II covers the important features of the new suspension and its general operating principles. Test results, including those obtained from strap-down drift tests and centrifuge tests, are discussed in Section III. Section IV is a detailed description of the circuitry; the procedure for adjusting and tuning the suspension is given in Section V. The reflected voltage problem, a major problem in suspension design, is covered in Section VI. Conclusions on the work to-date and recommendations for work to further advance electric vacuum gyro suspension circuit technology comprise Section VII.

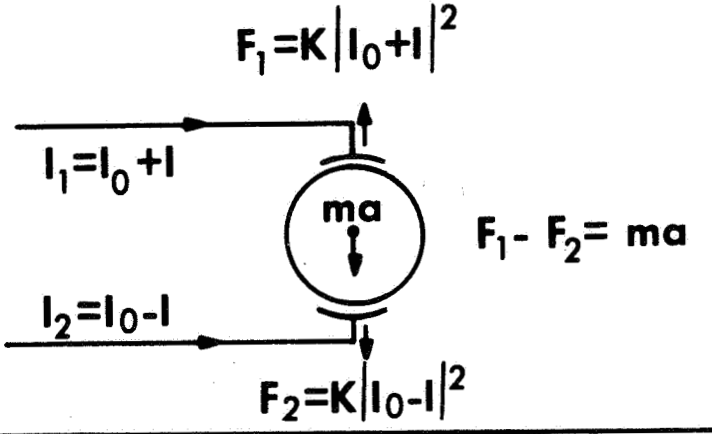

	AMPLITUDE MODULATION	PHASE MODULATION
VECTOR DIAGRAM	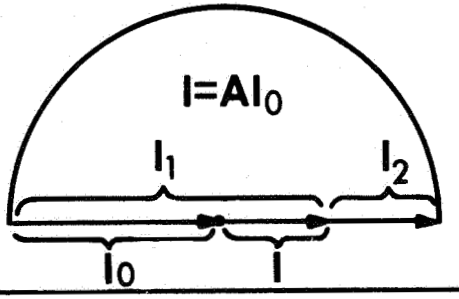	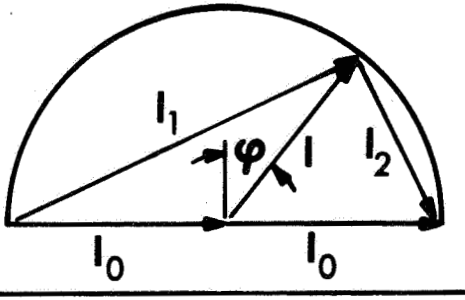
CONTROL VARIABLE	$A \quad (-1 \leq A \leq 1)$	$\varphi \quad (-90° < \varphi < 90°)$
RESULTANT FORCE $F_1 - F_2$	$4K\ I_0^2\ A$	$4\ K\ I_0^2 \sin\varphi$
SUM OF FORCES $F_1 + F_2$	$2\ K\ I_0^2\ (1+A^2)$	$4\ K\ I_0^2$ (CONSTANT)

Figure 1 Comparison of Amplitude and Phase Modulated Suspension

SECTION II
PHASE MODULATED SUSPENSION

The suspension circuitry developed under the present contract (Figure 2) has been built on cards for development convenience; no attempt has been made to package the circuitry compactly.

The main features of the suspension circuit are:

- Three suspension axes and three associated phases
- Carrier phase modulation
- Negative feedback of the electrode currents for stabilizing the current amplitudes
- Enhanced low frequency stiffness for good rotor centering
- Constancy of the sum of forces
- Rotor position error signal developed from the same carrier excitation as provides the force
- Error signal demodulated and compensated after demodulation
- Capability of operating over a range of excitation voltages and g-loadings

The phase modulation feature and its relation to the sum of forces constancy are illustrated in Figure 1.

The operation of the suspension circuitry can best be explained by referring to the block diagram (Figure 3) which shows its major functional components.

The system is powered from a variable voltage power supply. Varying the supply voltage changes the suspension g tolerance and also the power required. Each phase of the oscillator drives two current amplifiers, (I_o) and (I), which utilize negative feedback to attain a high output impedance. Rotor departure from center is sensed, demodulated, and compensated to provide adequate damping and

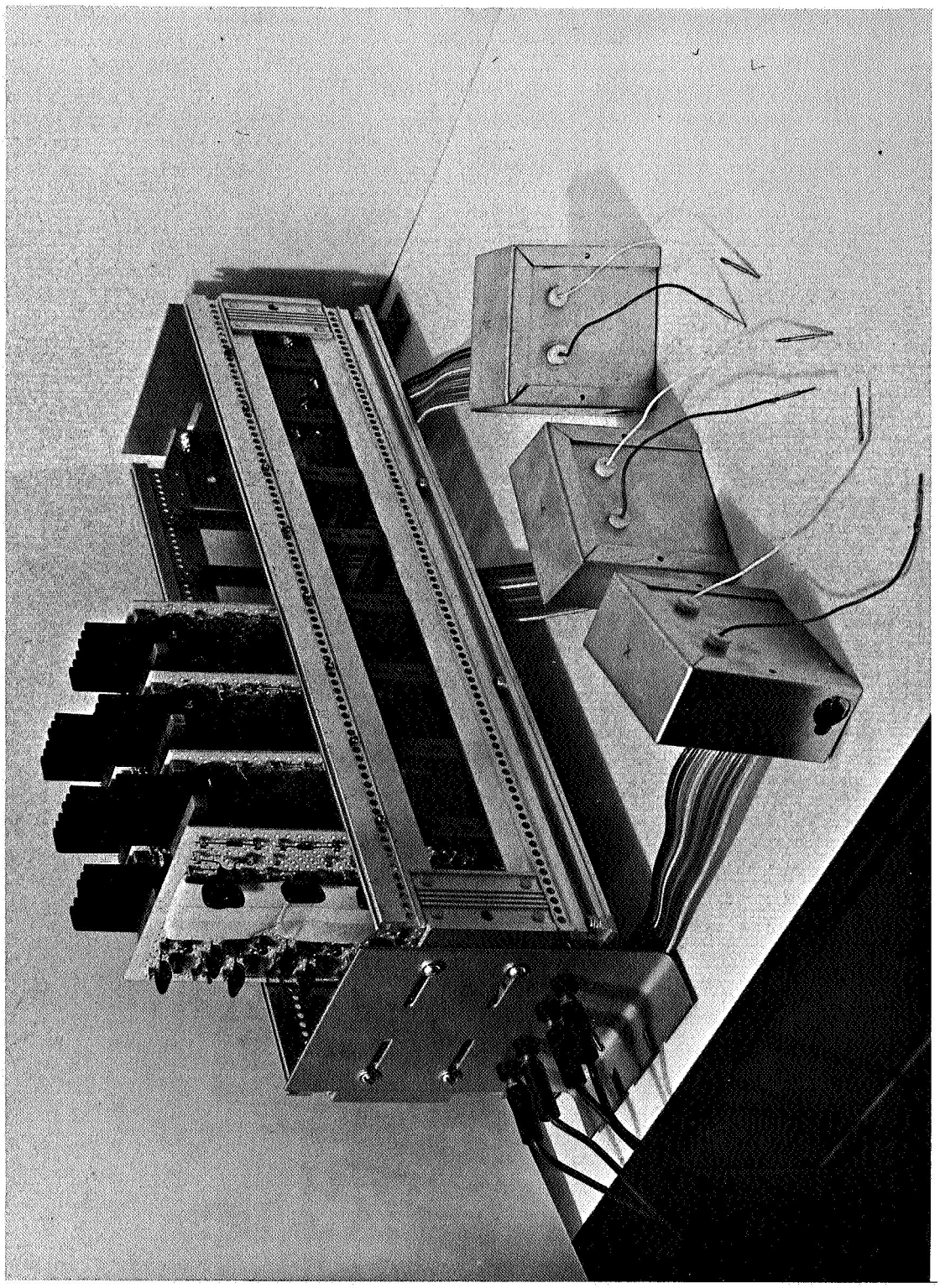

Figure 2 Phase Modulated Suspension

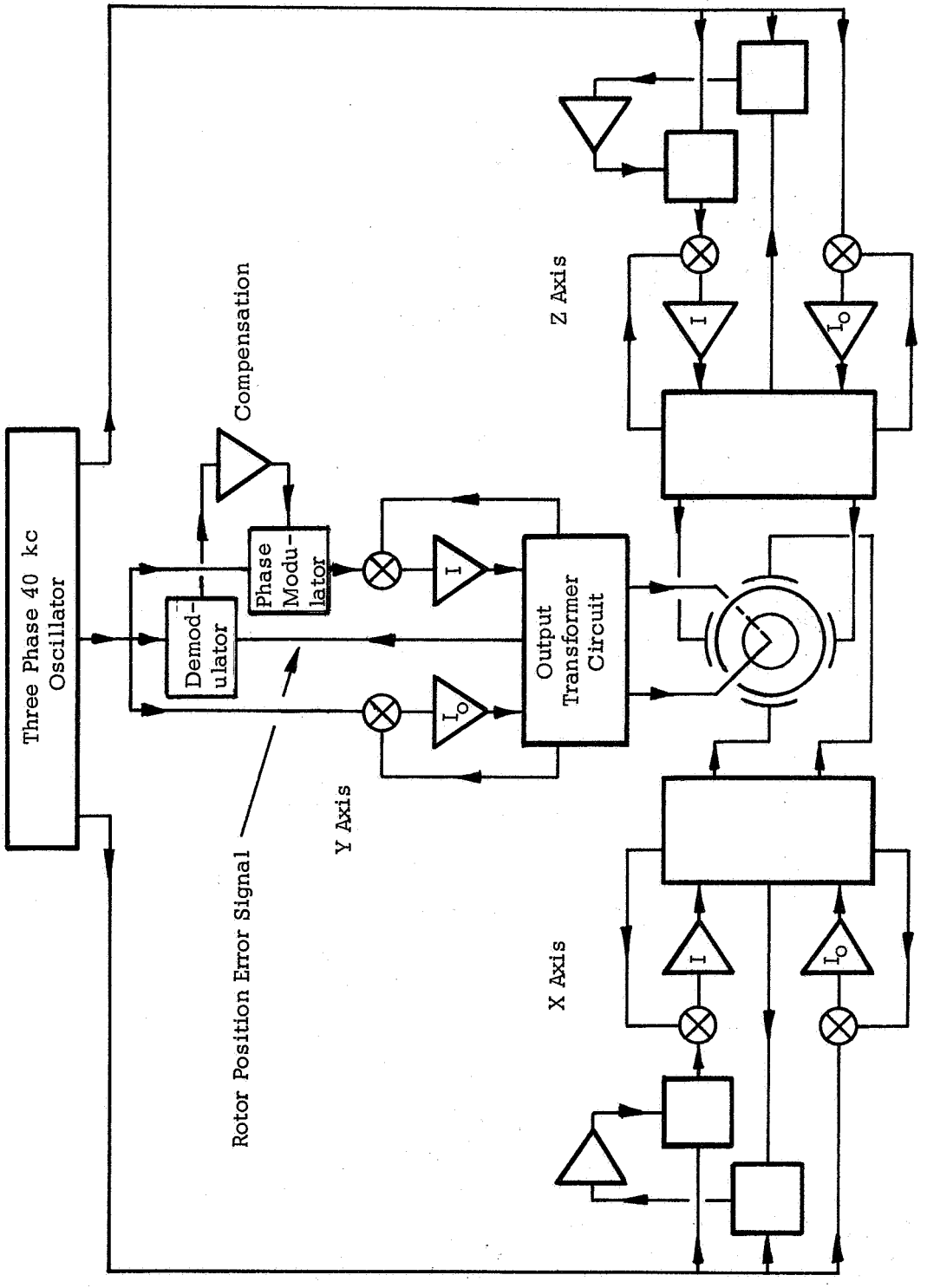

Figure 3 Block Diagram of Phase-Modulated Suspension

enhanced low frequency stiffness, and used to modulate the phase between the I and I_o amplifiers. The output of these amplifiers is summed in the output transformer circuit; the output of these transformers is applied to the suspension electrodes. Use of the balanced three-phase ac system maintains the rotor as a floating neutral.

SECTION III
SUSPENSION TESTS

GENERAL

Following successful development of the suspension circuitry, a series of tests was conducted to verify its predicted characteristics. These tests consisted of centrifuge tests to demonstrate the variable g capability of the suspension, and a strap-down gyro drift test to check the suspension under operation conditions. The results of these tests and the procedures followed are discussed in this section of the report.

CENTRIFUGE TESTS

Centrifuge tests were conducted to determine rotor deflection vs g loading, and the maximum g capability of the suspension at several values of supply voltage B_1. In all these tests the centrifugal loading was carried by one horizontal axis of the three orthogonal axes of the system, gravity loading by another, while the third axis remained unloaded.

Results of the tests are shown in Figure 4. The sloping straight lines are best fits to the measured values, and show approximately the expected increase in stiffness with increasing B_1. The gap is 2,000 microinches (on the radius), so that it is apparent from Figure 4 that the rotor remains centered within 4% of the gap for all g loadings short of failure.

Figure 5 (a) shows the measured electrode current I_o as a function of the B_1 supply voltage. From the electrode current values, the electrode area, and the rotor mass, one can compute the maximum g capability of the phase modulation system, with the results shown as the solid curve of Figure 5 (c). In making this theoretical estimate, account must be taken of two separate correction factors, namely, that the individual electrodes of a connected pair exert

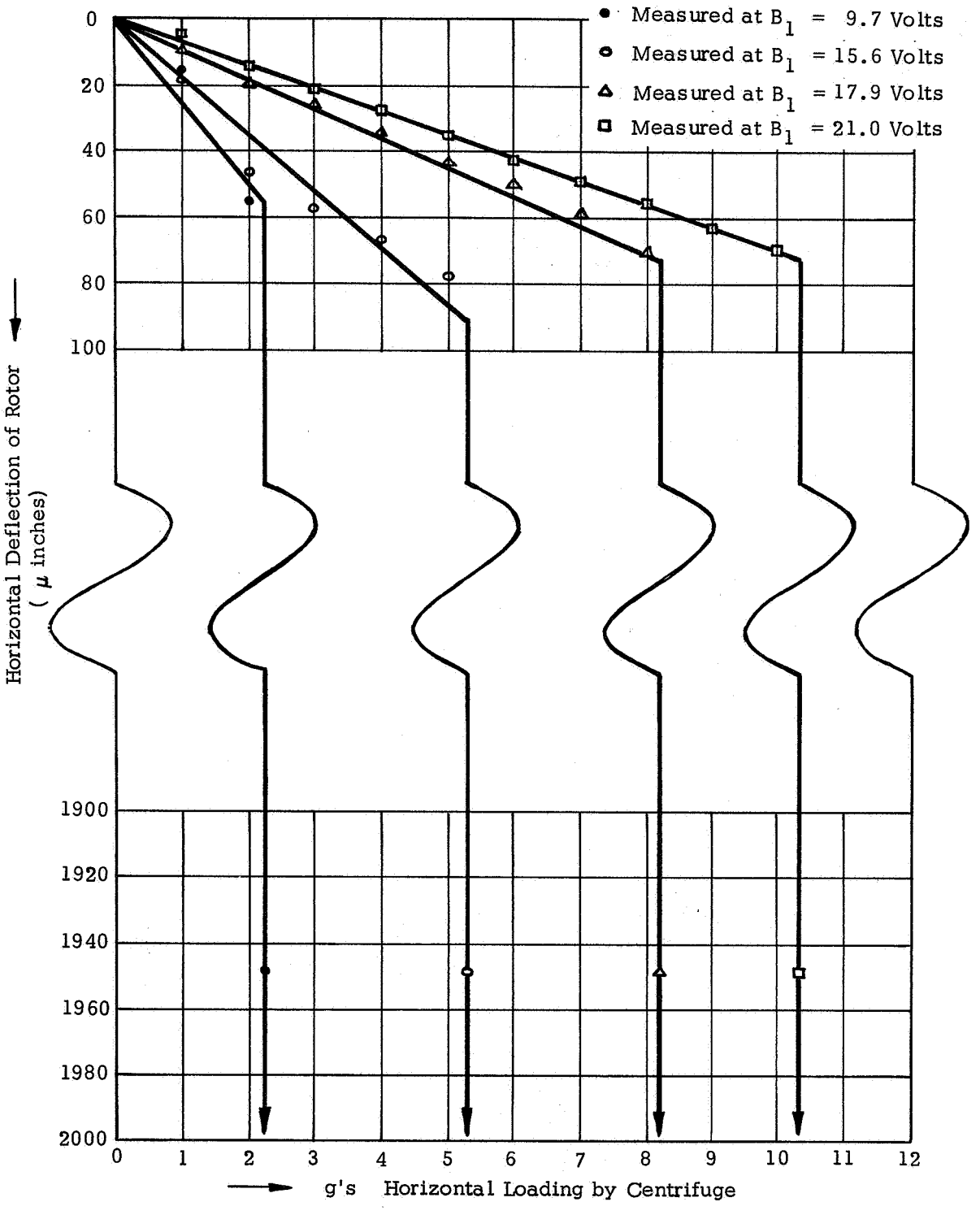

Figure 4 Centrifuge Test Results

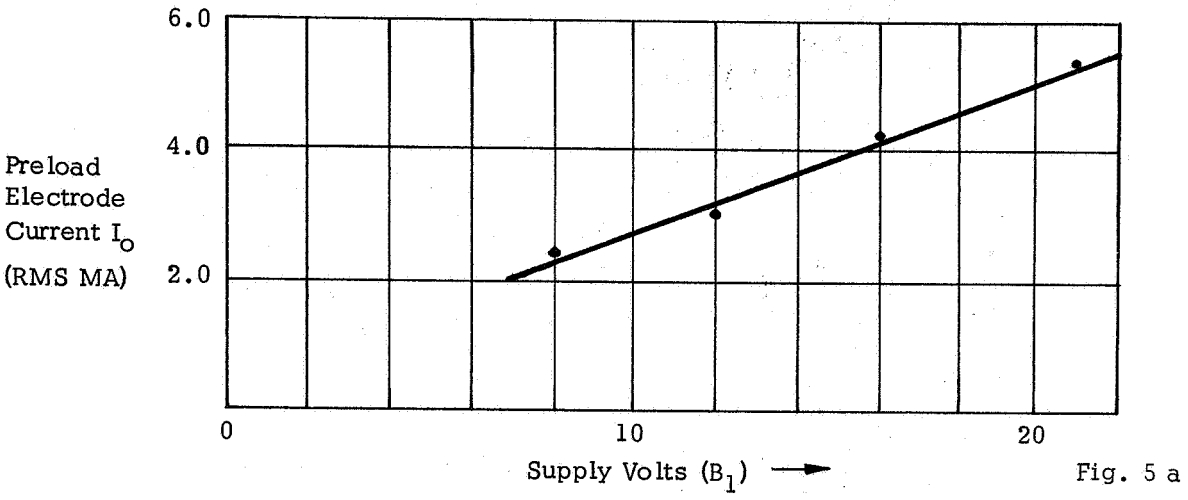

Fig. 5 a

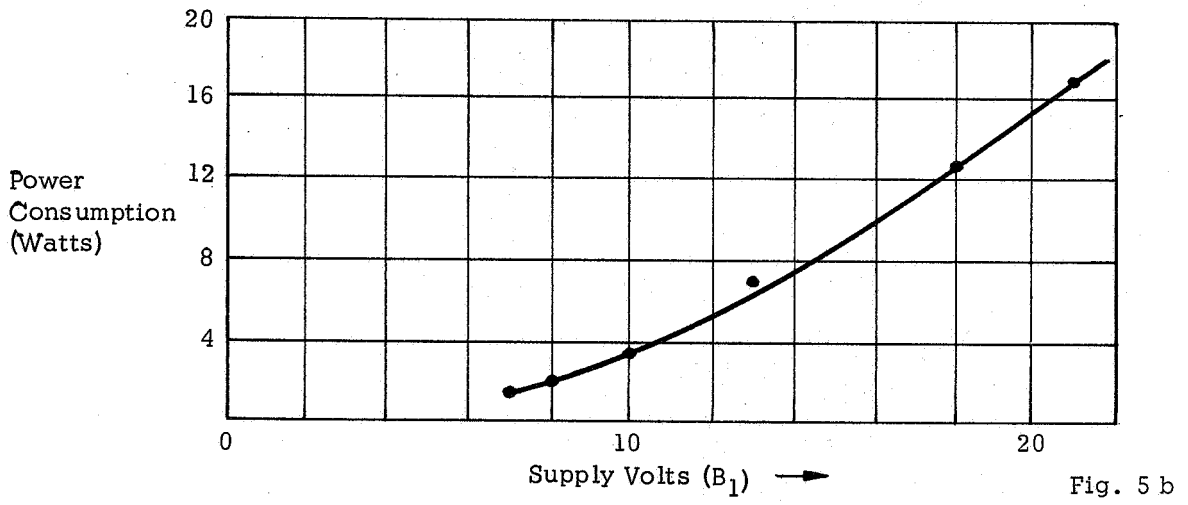

Fig. 5 b

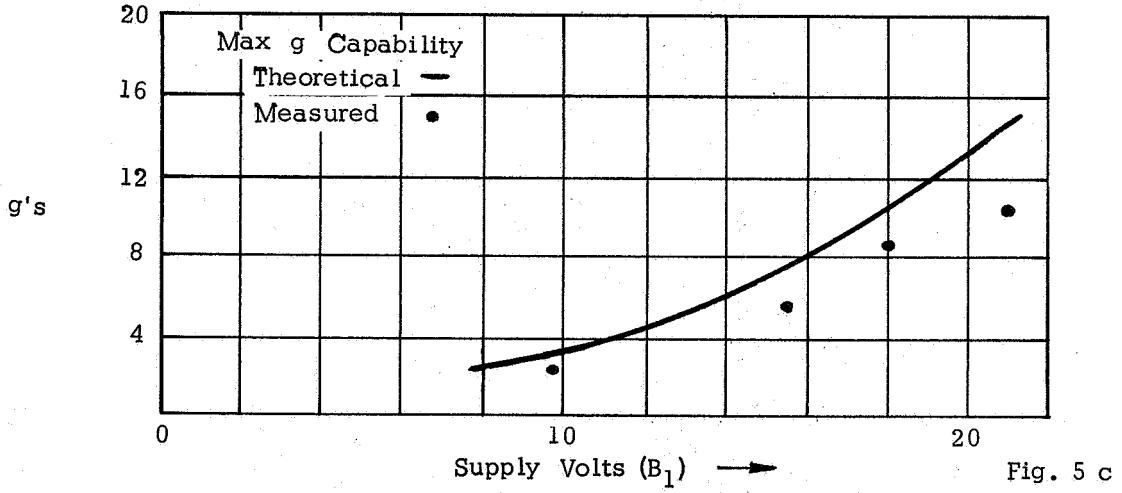

Fig. 5 c

Figure 5 Suspension Electrical Characteristics

forces at an angle of 32^{o} to the corresponding axis leading to a correction factor of cos 32^{o} = .85, and that as the phase of I approaches that of I_o the force saturates and the incremental stiffness tends to zero leading to a correction factor estimated at 0.80. The observed maximum g capability falls below the theoretical, as it must, but only about 25% at the higher g loadings.

Figure 5 (b) gives an idea of the total power consumption to be expected in an operating suspension circuit of this type. The power figures are somewhat arbitrary since in actual operation the value of B_2, the push-pull amplifier supply, is supposed to be adaptively controlled independent of B_1, and most of the current drain is from B_2. In the absence of operating experience with B_2 adaptively controlled, we have arbitrarily put $B_2 = 1/2\ B_1$, which is a workable, but probably not optimum, relationship between the two supply voltages. On this basis, it is predicted that for this suspension system the power consumption will range from about 1.5 watts to 17 watts as the imposed g loading varies from 1g to 12g.

The centrifuge tests were performed using a Trio-Tech Model G-269-0 Centrifugal Accelerator driven by a hydraulic power unit and capable of providing accelerations in the 1 to 200-g range. The gyro was mounted at a radius of 47.63 inches with centrifugal accelerations acting along the suspension z axis. Electronics were mounted at a smaller radius and cable connected to the gyro since they were mounted on cards and not packaged to withstand high accelerations. The suspension power supply was mounted externally to the centrifuge to facilitate power measurements. Rotor displacement signals were brought out of the centrifuge via buffer amplifiers and slip rings.

STRAP-DOWN DRIFT TEST

A strap-down test was conducted on an EVG to check out the suspension circuitry under operating conditions. Approximately 2.5 hours were used to bring the rotor up to its operating speed (800 rps) and actuate the readout and data acquisition equipment; 65 hours were used in a drift test. Normal spin-up time is 1 minute, but the long spin-up time was required to observe suspension behavior at various

rotor speeds. A mild instability was noted on one suspension axis during spin-up and corrected by adjusting the coefficient for that axis. Time did not permit further investigation to determine why the one axis differed from the other two.

Drift information was obtained from the data by using a digital computer to make a least squares fit of a Fourier series to the first 22 hours of data after spin-up, and using this series to predict rotor position for the balance of the run. Fourier coefficients and differences between predicted and actual data are given in Figures 6 and 7.

The constant term and the first two Fourier harmonics can normally be translated to g insensitive, g, and g^2 type coefficients by use of a mathematical model for the gyro but, due to the condition of the rotor in the gyro used, this interpretation is difficult. The only gyro available for the test was one with a rotor badly scarred by suspension experiments. The poor condition of the rotor is evidenced by the poor drift results and the relatively large high-order Fourier harmonics; with a normal rotor, all harmonics above the second are down in the noise level.

In the strap-down gyro test, the gyro case was fastened to a rigid base. The rotor spin axis remained fixed in direction in space except for drift, and the gyro case rotated with the earth. Readout data from two axes was automatically read and recorded.

The test stand used includes a pedestal, a two-axis table for adjusting the gyro to any desired angle, a data acquisition system, a key-punch machine for recording the test data, and a Hewlett-Packard 5243L electronic counter for measuring rotor speed.

The pedestal to which the turntable is mounted is a concrete pillar bolted rigidly to the floor. The top of the pedestal is stable to within approximately 5 arc seconds.

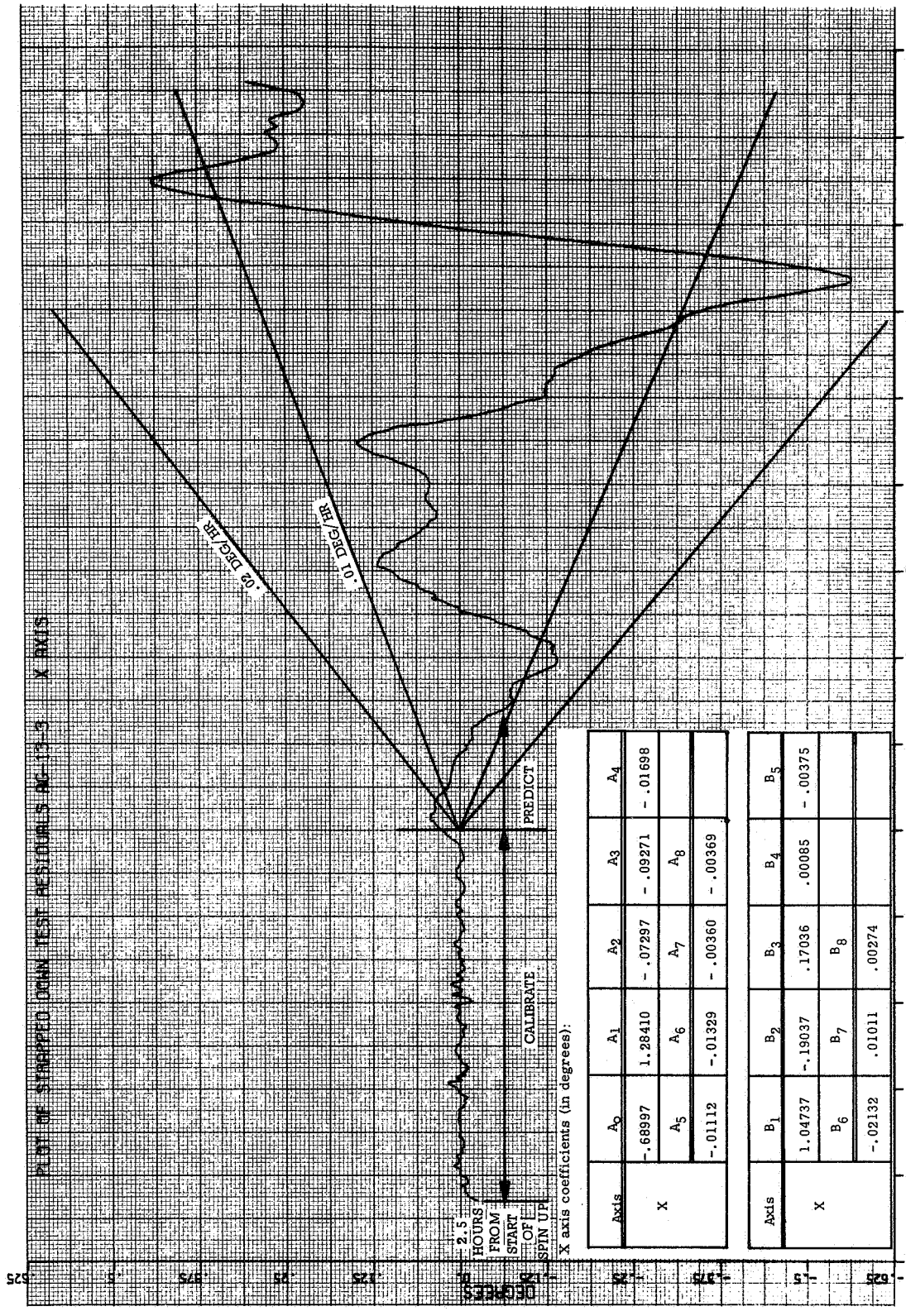

Figure 6 Strap Down Test Results (x axis)

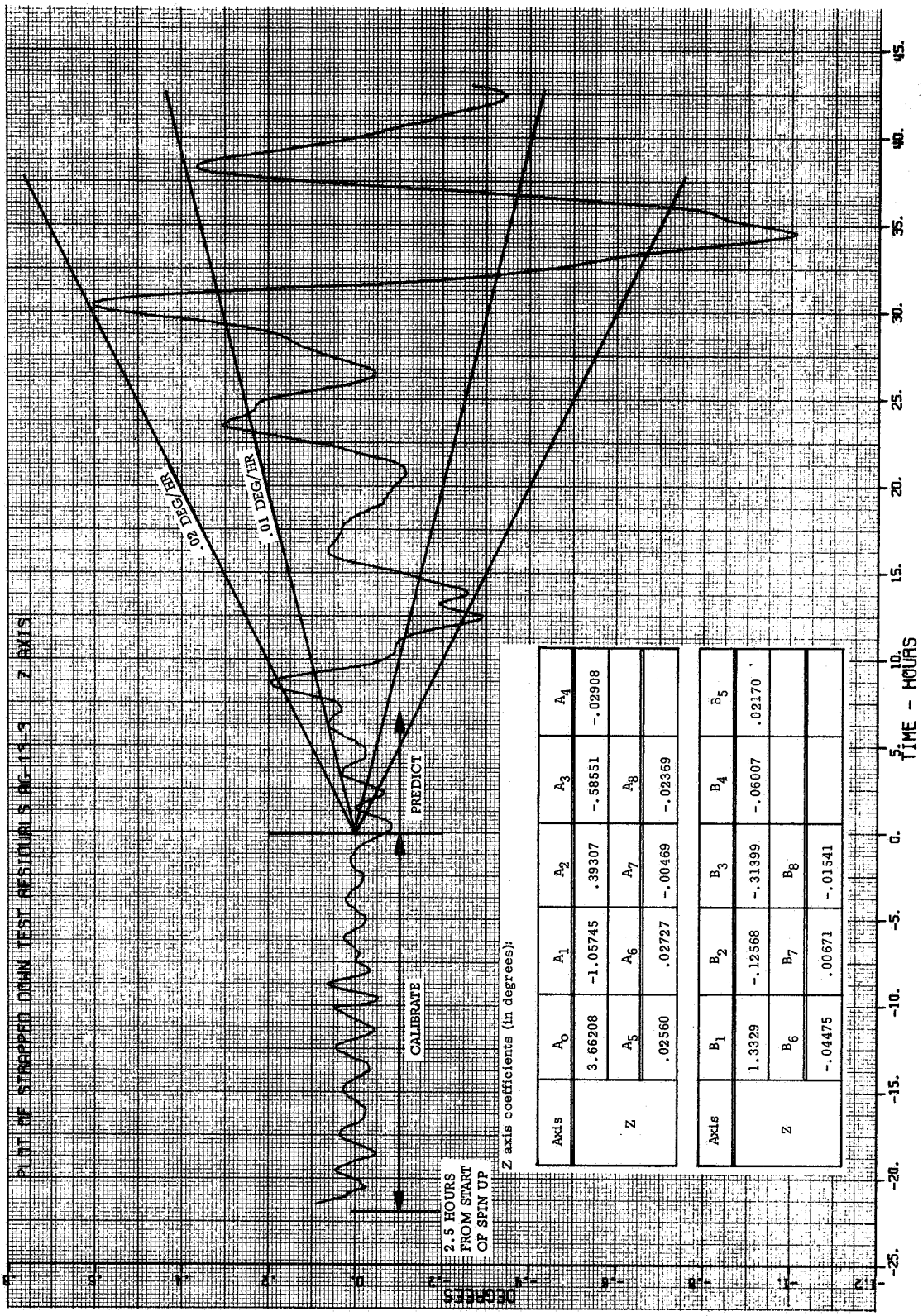

Figure 7 Strap Down Test Results (z axis)

The two-axis table used to position the gyro is a Bowcan Model B-94 table made of aluminum. The table top angle can be read to 15 arc seconds and the elevation angle can be read to 30 arc seconds. These readings were used to align the gyro approximately, but final adjustment of gyro angles was made using autocollimating theodolites and reference mirrors mounted on the gyro.

The data acquisition system accepts readout data from the gyro, converts it to digital form, and then transfers the information to an IBM key-punch machine which automatically records the data in a form which facilitates analysis.

The procedure in the strap-down drift test was as follows: The gyro was mounted on the test stand, and a case axis was lined up with the gyro Y axis parallel to the earth's axis with +Y North, and the gyro X axis horizontal with +X West. The angular momentum vector (H, in the mathematical model) and the mass unbalance vector were along the -Y axis. The suspension system was turned on (excitation voltage: 10 vdc) and checked for damping, stiffness, rotor centering, and sum of forces constancy. Spin-up torque was then applied sufficient to bring the rotor up to a low speed for check of readout signals. Finally, the rotor was spun up to operating speed (800 rps) and the automatic readout data recording was started. The combination of spin-up torque misalignment with the case axis, and mass unbalance torque and pattern torque, resulted in an initial condition of about 1.5^{o} cone half-angle, and the gyro was allowed to operate on the cone determined by these conditions. The mathematical model used in analyzing data was:

$$H_{x,y,z}(\text{Deg}) = A_o + \sum_{n=1}^{8} A_n \cos\ n\Omega t + B_n \sin n\Omega t$$

where the fundamental period is 21.78 hours.

SECTION IV
DESCRIPTION OF SUSPENSION CIRCUIT

CIRCUIT DEVELOPMENT CONSIDERATIONS AND ENGINEERING SELECTIONS

The important engineering selections in the circuit development are discussed below. In considering each individual design problem, careful attention was given to its compatibility with the integrated system design.

Choice of Carrier Frequency

A 40-kc frequency was selected because this frequency has been convenient in all previous EVG suspension work. It is the lowest frequency with adequate clearance relative to rotor rotation and vibration frequencies which may range up to 1 or 2 kc.

Choice of Transistor Types

After a survey of commercially available types, two complimentary silicon transistor types were chosen, the 2N930 (NPN) and the 2N2907 (PNP). Silicon was preferred over germanium for temperature and bias stability and military compatibility. These two types can perform all required functions, with more than adequate frequency response, derated one-half in voltage and one-tenth in both current and power dissipation. A compatible silicon diode, the 1N625, was selected to perform all the diode functions.

Choice of Supply Voltage Range

Since the supply voltage must have reliability comparable with that of a storage battery, and since the transistor voltage limitation is about 45 volts, the maximum supply voltage was chosen to be approximately 21 volts. The minimum voltage would be about 7 volts, resulting in a 9-fold range of g tolerance. Below 7 volts it becomes difficult, in the circuit design, to allow for the silicon diode forward voltage drop of about 0.6 volt.

Means for Varying the Supply Voltage without Wasting Power

Starting from a storage battery primary supply at fixed voltage of 24 to 28 volts, a dc-to-dc converter to supply a voltage, electronically adjustable from 21 volts down to 7 volts, is required. A standard circuit for doing this can be used but has not been constructed.

Choice of Waveform for Push-pull Output Amplifiers

Sine waveform is employed in the final circuit, since sine waves are compatible with the phase modulator that was developed.

Three-Phase Oscillator Design

A very satisfactory oscillator has been in use since early 1966. The oscillator circuit is described later in this section.

Output Transformer and Resonating Reactor Design

Ferrite cores are used in the output transformers with a high voltage winding of 900 turns, and primary windings of 45 turns for a voltage step-up of 20:1. Earlier, a step-up of 5:1 was tried but caused trouble from the "reflected voltage" problem, discussed in Section VI. A molybdenum permalloy powder core resonating reactor is used.

Circuit for Sensing Rotor Displacement

This circuit is a direct adaptation of that used on the Mod 0 suspension and functions well, providing about 500 volts PTP per inch. More volts per inch would be desirable, and could be provided with some circuit modification.

Demodulation and Compensation of Rotor Displacement Signal

A conventional, balanced full wave diode bridge rectifier is used. All the compensation is done in one dc stage with resistors and capacitors only. There is a lag network in the base circuit and a lead-lag network in the emitter circuit and in the collector circuit.

Phase Modulation Scheme

The function of the phase modulator is to drive the I push-pull amplifier (at constant amplitude) with phase determined by the compensated rotor displacement signal, thus supplying a restoring and damping force to the rotor. This is clearly a critical item in the overall circuit and it must involve a nonlinear control element. Consequently, intensive investigation of various phase modulation schemes was made. Most voltage-controlled resistor schemes, tunable reactor schemes, and variable transistor storage delay time schemes were experimented with. Voltage controlled capacitors and light-controlled resistors were also considered.

The main problem was to make a variable component, either pure resistive or pure reactive, which remained "pure" enough while the magnitude was varied. If the supposedly pure variable resistor, for example, developes some reactance while being modulated, the result is amplitude modulation superposed on the desired phase modulation, which spoils the sum of forces constancy.

The final satisfactory solution to the phase modulation problem is in the form of a variable pure resistor created by starting with a parallel resonant circuit and degrading its shunt resistance progressively by variable negative feedback. This arrangement permits modulating the phase $\pm 70^{o}$, with amplitude variation less than 1%. The quoted range of phase is as much as can be used in the suspension circuit. The circuit details are described later in this section.

Electrode Current Feedback Scheme

The waveform and amplitude constancy of suspension electrode currents can be improved through the use of negative feedback. By means of a center-tapped transformer the sum $(2\,I_o)$ and difference $(2\,I)$ of the electrode currents are caused to develop voltages across two resistors. These voltages, in turn, are summed, with a negative sign, into the I_o amplifier and I amplifier drives.

Reflected Voltage Problem

The reflected voltage problem was discussed in detail in the third quarterly progress report. The solution proposed therein has been found effective and is employed in the present circuit. The discussion of reflected voltage is included in this report as Section VI.

DESCRIPTION OF THE PRINCIPAL ELEMENTS OF THE SUSPENSION SYSTEM

General

The principal elements of the suspension system are the three-phase oscillator circuit, the suspension feedback loop, and the output transformer circuit. The oscillator circuit is common to the three axes of the suspension system. Each of the three axes contains a suspension feedback loop and an output transformer circuit. The complete suspension system is shown in Figure 8. The principal elements are discussed in the paragraphs following, and illustrated in Figures 9, 10 and 11.

Three-Phase Oscillator Circuit

The oscillator circuit (Figure 9) consists of three identical push-pull sections operating 120° apart in phase. The tank coil windings have their center taps returned to ground. A pair of driving transistors (e.g., Q_{17} and Q_{18}) operate as a differential positive feedback amplifier, switching a substantially constant current from side to side at the input to the tank circuit. The oscillator level is set by the amount of current being switched which, in turn, is determined by the common dc base bias of all six transistors Q_{17} through Q_{22}. Q_{16} supplies this dc bias and is adjusted so that Q_{17} through Q_{22} operate just short of saturation. The three sections are coupled together in a ring configuration, each section driving the neighboring section via two R-C networks which shift the phase 60°. Taking the 180° phase reversal between transistor base and collector into account, this provides a net 120° phase separation between sections.

The oscillator starts up from noise very rapidly (within 2 or 3 cycles) and reliably, and holds a constant amplitude, proportional to the B_1 voltage and

A1

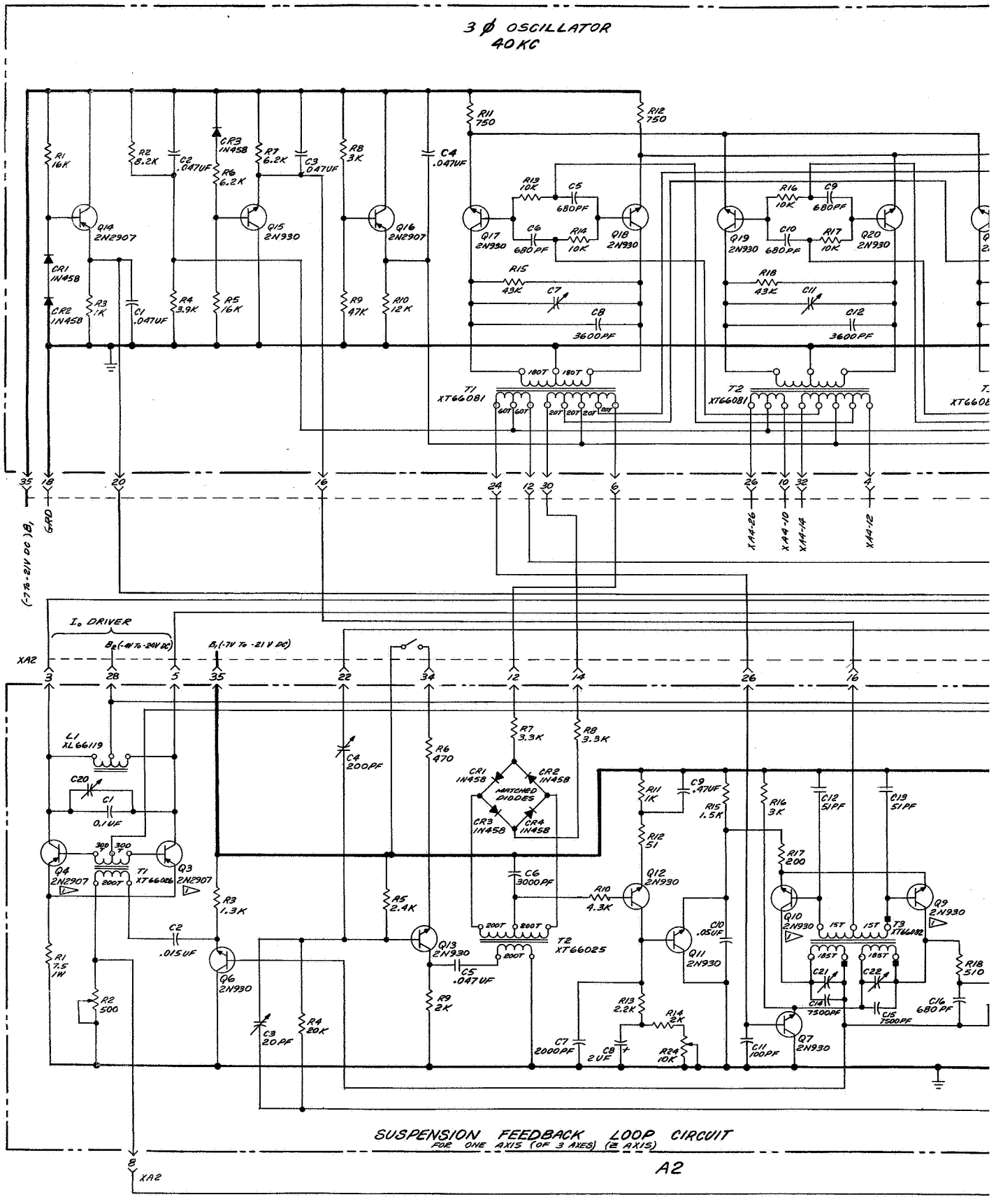
3 Ø OSCILLATOR
40KC
R1 16K
R2 8.2K
C2 .047UF
CR3 1N458
R6 6.2K
R7 6.2K
C3 .047UF
R8 3K
C4 .047UF
R11 750
R12 750
Q14 2N2907
Q15 2N930
Q16 2N2907
R13 10K
C5 680PF
C6 680PF
R14 10K
Q17 2N930
Q18 2N930
R16 10K
C9 680PF
C10 680PF
R17 10K
Q19 2N930
Q20 2N930
CR1 1N458
CR2 1N458
R3 2.1K
C1 .047UF
R4 3.9K
R5 16K
R9 47K
R10 12K
R15 43K
C7
C8 3600PF
R18 43K
C11
C12 3600PF
T1 XT66081
T2 XT66081
180T 180T
60T 60T 20T 20T 20T
35 18 20 16 24 12 30 6 26 10 32 4
GRD
(-7 TO -21V DC) B1
XA4-26
XA4-10
XA4-14
XA4-12
I₀ DRIVER
B2 (-14 TO -24V DC)
B1 (-7V TO -21 V DC)
XA2
3 28 5 35 22 34 12 14 26 16
L1 XL66119
C20
C1 0.1UF
30P 300
Q4 2N2907
T1 XT66026
200T
Q3 2N2907
R3 1.3K
C2 .015UF
R1 7.5 1W
R2 500
Q6 2N930
C4 200PF
R6 470
R7 3.3K
R8 3.3K
CR1 1N458
CR2 1N458
MATCHED DIODES
CR3 1N458
CR4 1N458
C6 3000PF
R5 2.4K
Q13 2N930
C5 .047UF
200T 200T
T2 XT66025
R9 2K
C3 20.PF
R4 20K
C7 2000PF
C8 2UF
R24 10K
R10 4.3K
Q12 2N930
R11 1K
C9 .47UF
R15 1.5K
R12 51
Q11 2N930
C10 .05UF
C11 100PF
R13 2.2K
R14 2K
R16 3K
R17 200
C12 51PF
C13 51PF
Q10 2N930
Q9 2N930
15T 15T
T3 XT66082
185T 185T
C21
C22
C14 7500PF
C15 7500PF
C16 680 PF
R18 510
Q7 2N930
SUSPENSION FEEDBACK LOOP CIRCUIT
FOR ONE AXIS (OF 3 AXES) (Z AXIS)
A2
8
XA2

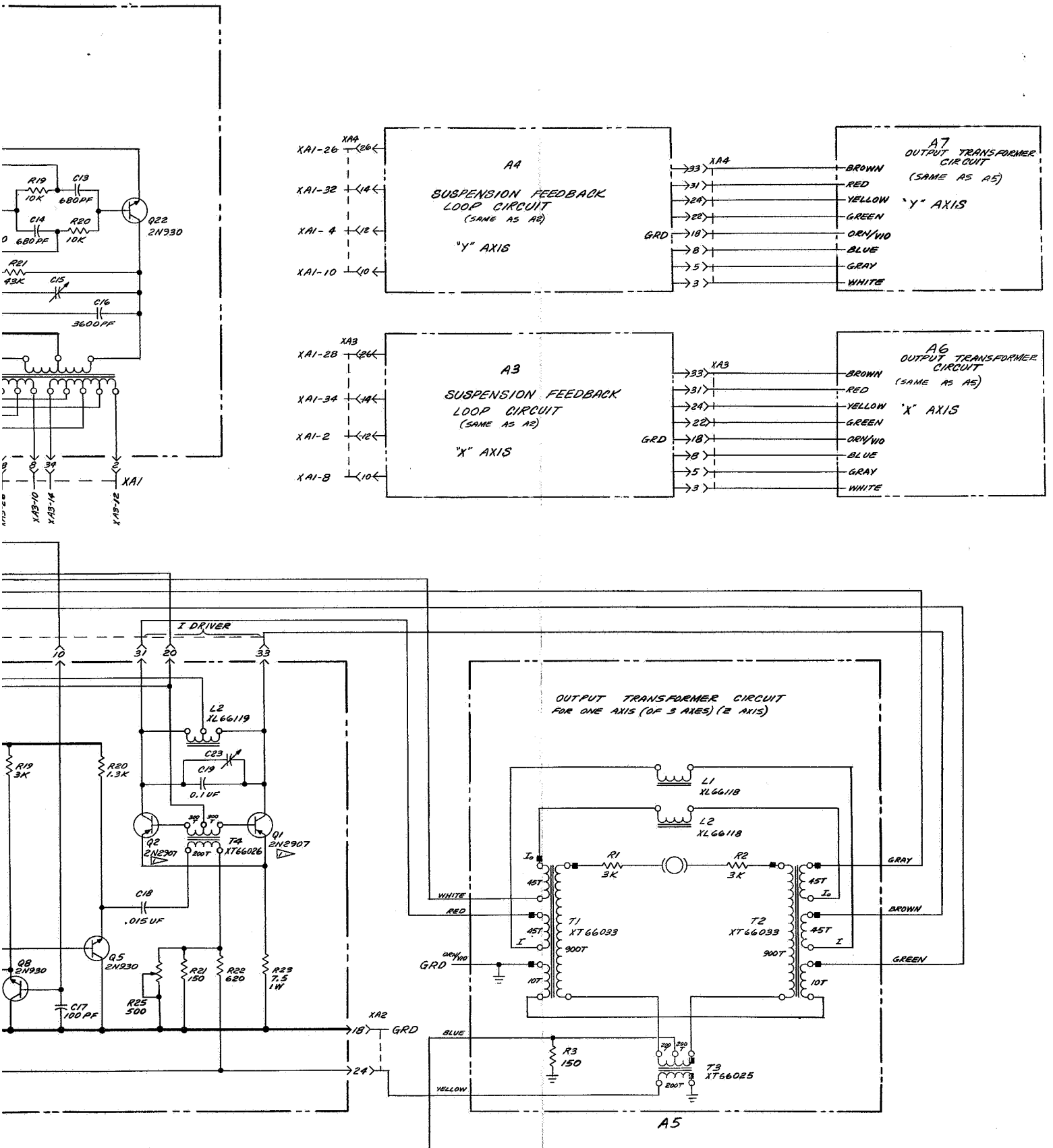

Figure 8 Suspension System Schematic

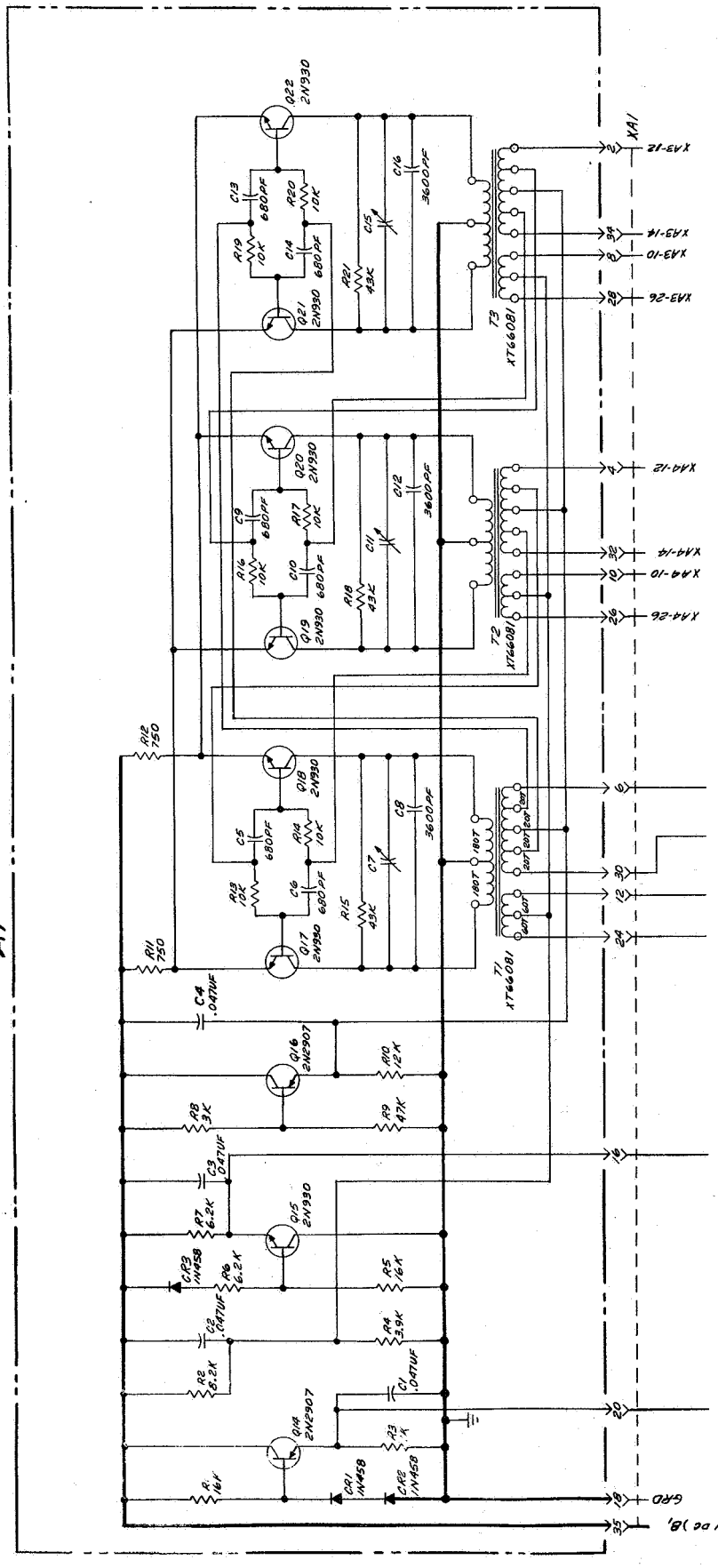

Figure 9 Three-Phase Oscillator Schematic

variable with it, keeping a pure sine waveform throughout. The use of only two emitter resistors as shown, rather than one for each section, improves the efficiency and the waveform. The oscillator draws about 2 mA at $B_1 = -12$ volts.

The feedback windings are extended (terminals 6, 30, etc.,) to provide an appropriately biased ac output for driving diode synchronous rectifiers for error signal demodulation (Figure 10). Still another winding with separate dc bias (terminals 12, 24, etc.,) is provided on each tank coil for driving the I_o amplifier and the phase modulator (Figure 10). The R_2,R_4 resistor divider supplies this latter bias.

Two bias circuits (Figure 9), which have nothing to do with the oscillator, are placed on the same subassembly only because, like the oscillator, they are common to the whole suspension. Q_{15} provides a common bias for the phase modulator control circuits and Q_{14} a common bias for the push-pull amplifier bases to minimize crossover distortion in those amplifiers.

The oscillator will operate over a range of B_1 voltages from about -4 volts to -25 volts, and over the range of -7 to -21 volts actually used the frequency remains within the range 400,000 ± 0.020 kc., which is better carrier frequency stability than required, since the most frequency-sensitive element in the suspension circuit has a bandwidth of about 1.5 kc. Temperature dependence of frequency is ± .2% between -65°F and $+160^{\circ}$F, which is quite tolerable.

Adjustment of the oscillator is described in Section V.

Suspension Feedback Loop Circuit for One Axis

A circuit (Figures 10 and 11) is associated with each phase of the oscillator and with each Cartesian axis of rotor linear displacement. The main function of the circuit is to sense displacement along that axis and provide restoring force. The circuit of Figure 10 provides two outputs, both of constant amplitude and one of fixed phase (I_o) and one of variable phase (I), which are then added and subtracted in the two output transformers of Figure 11 to achieve the effect illustrated in the diagram of Figure 1.

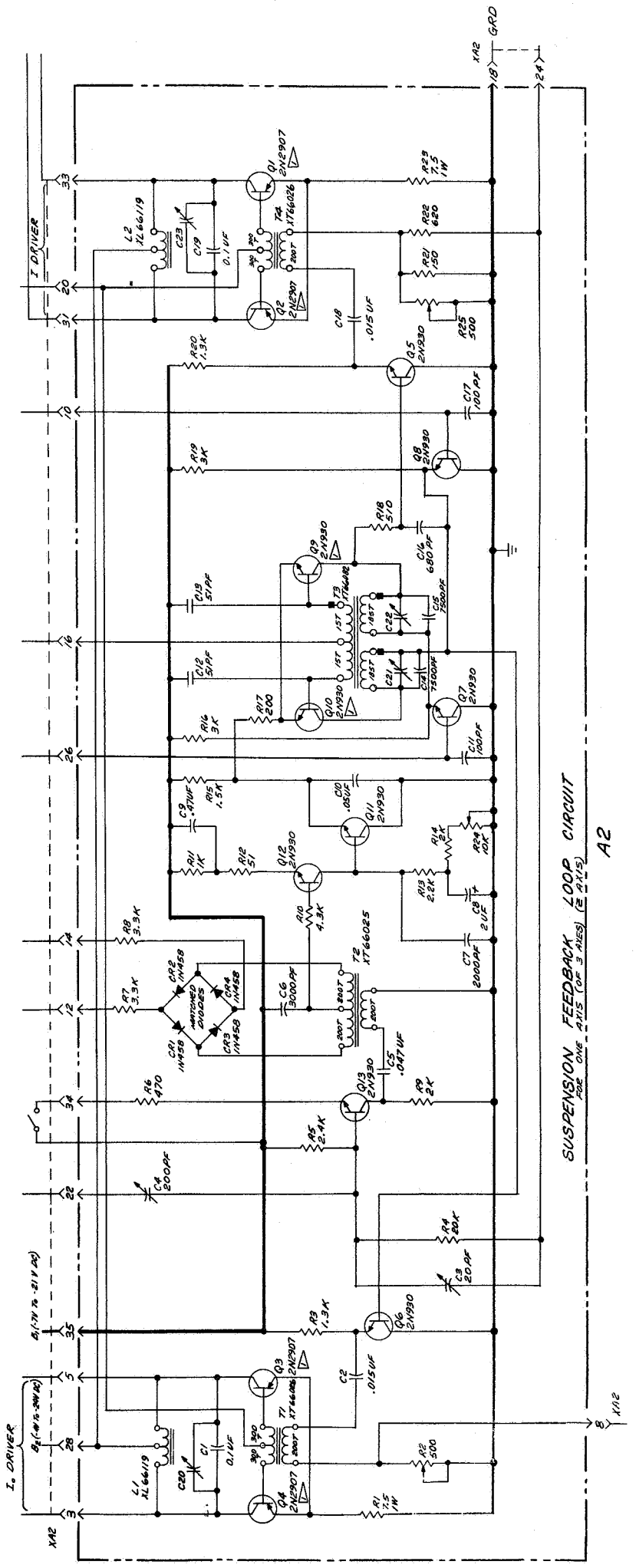

Figure 10 Suspension Feedback Loop Schematic

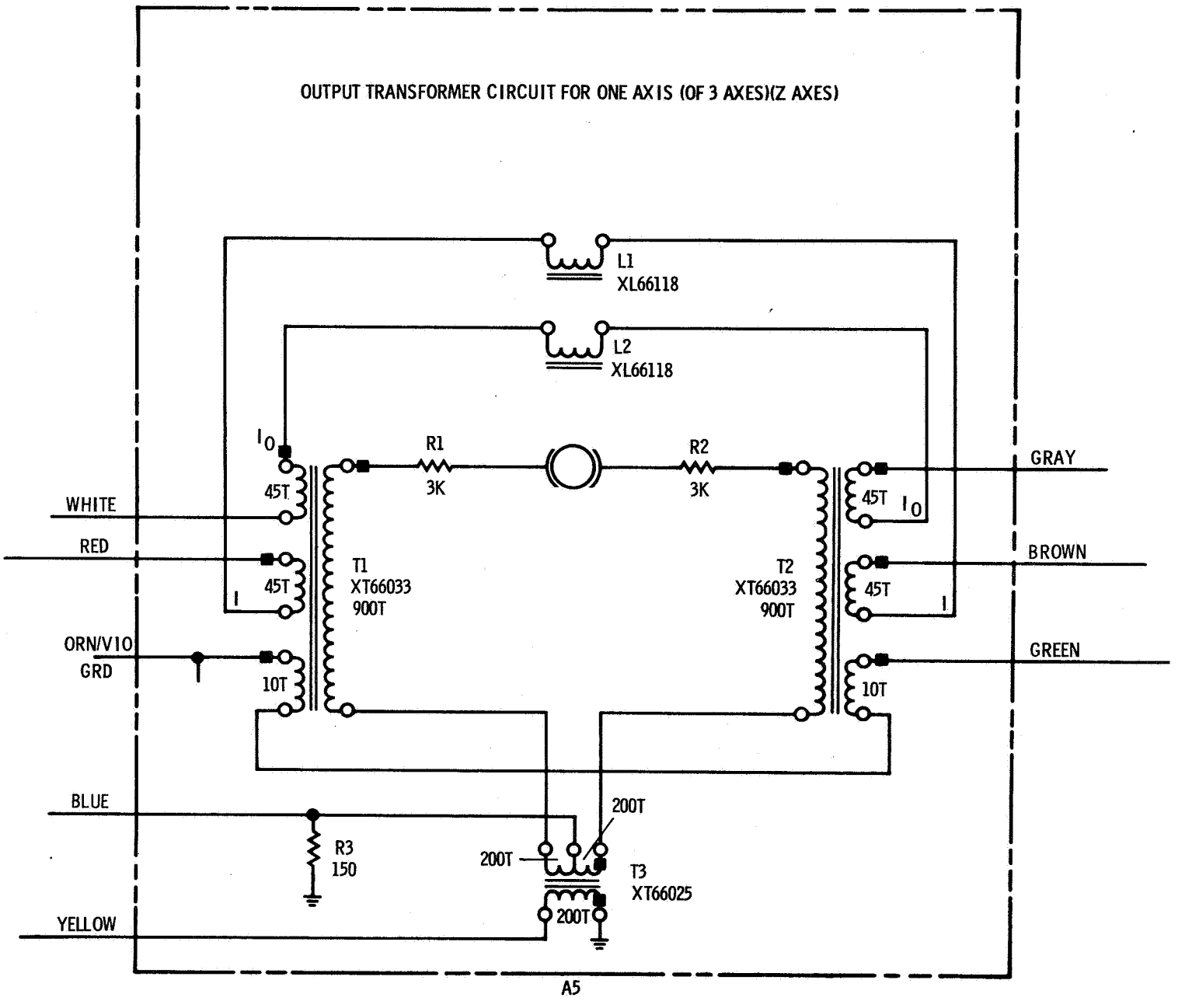

Figure 11 Output Transformer Schematic

The fixed phase output from the circuit of Figure 10 is developed simply by driving the output class-B push-pull amplifier (Q_3 and Q_4) from the emitter follower stage Q_6, the latter from emitter follower stage Q_8, and the latter from the oscillator. The electrode current from this amplifier chain tends to be quite independent of load because of the high collector impedance of the push-pull amplifier. The electrode current is further stabilized with respect to changes of load by a negative feedback loop as follows: The sum of the electrode currents, which is what this amplifier chain produces, developes a voltage across the R_3 resistor (Figure 11), and that voltage on terminal 8 subtracts from the push-pull drive voltage. Thereby, the output impedance is approximately doubled.

The electrode current waveform is improved and the push-pull amplifier load impedance lowered by providing in the load circuit, a parallel resonant circuit L_1 and C_1 of Figure 10 and a series resonant circuit L_2, and the electrode capacitance reflected through the output transformer of Figure 11. The shunt impedance across the push-pull collective terminals 3 and 5 is about 40 ohms, and nearly pure resistive.

The variable phase output is generated by an identical amplifier chain with negative feedback, consisting of push-pull amplifier Q_1 and Q_2, and emitter follower stage Q_5. However, Q_5 is driven by the output of a phase modulator to be described.

The oscillator drives emitter followers Q_7 and Q_8, 180^o out of phase and at the same level. Between the emitters of Q_7 and Q_8 is connected a series combination of a capacitor (C=680 pF) and a voltage-controlled variable resistor designated R, to be described. Given the variable R, it follows from Kirchoff's laws that the voltage at the junction point of R and C (base of Q_5) has a constant level equal to the common level at the Q_7 and Q_8 emitters, and a phase relative to the phase at the Q_7 emitter given by

$$\varphi = 2 \arctan (\omega RC)$$

where ω is the carrier radian frequency. Thus, φ can be modulated by modulating R. In practice, the range of φ is: $20^{o} \leq \varphi \leq 160^{o}$. The constancy of amplitude level of the phase-modulated signal requires that the loading of the junction point of R and C be negligible, and that R remain a purely resistive element as its magnitude is varied.

R is made up of a small fixed resistor R_{18} and the shunt impedance of a parallel resonant circuit accurately tuned to the carrier frequency. The parallel resonant circuit is configured so that a balanced amplifier Q_9, Q_{10}, can be coupled to it in negative feedback fashion to lower its shunt impedance by a controlled amount. This configuration is substantially the same as that of an oscillator section of Figure 9 except for reversed polarity of feedback. A direct current of amount controlled by Q_{11} is switched from side to side of the resonant circuit by Q_9 and Q_{10} acting as a differential amplifier.

Q_{11} is driven by the demodulated and compensated rotor position error signal, so that the phase of I and consequently, the force, is controlled by the rotor displacement. Q_{11} and Q_{12} are dc amplifier stages. All of the compensation is performed in the Q_{12} stage which has a lag network in the base circuit, and a lead-lag combination in the emitter circuit and in the collector circuit. The collector lead-lag provides enhanced low frequency stiffness in the region from about 10 cps downward. The lead-lag in the emitter circuit provides damping between about 100 cps and 4,500 cps, and in the designed range of resonant frequencies, 300 cps to 900 cps (depending on the excitation level), the damping is better than 1/2 critical damping. Figure 12 exhibits the designed gain and phase characteristic of the compensation amplifier and the phase characteristic measured on the actual circuit.

The rotor position error signal, originally generated at the collector of Q_{13} in the form of an amplitude-modulated 40-kc carrier, is synchronously demodulated by the diode full wave bridge, terminals 12 and 14 being driven by the oscillator. The demodulated signal feeds the base of Q_{12}.

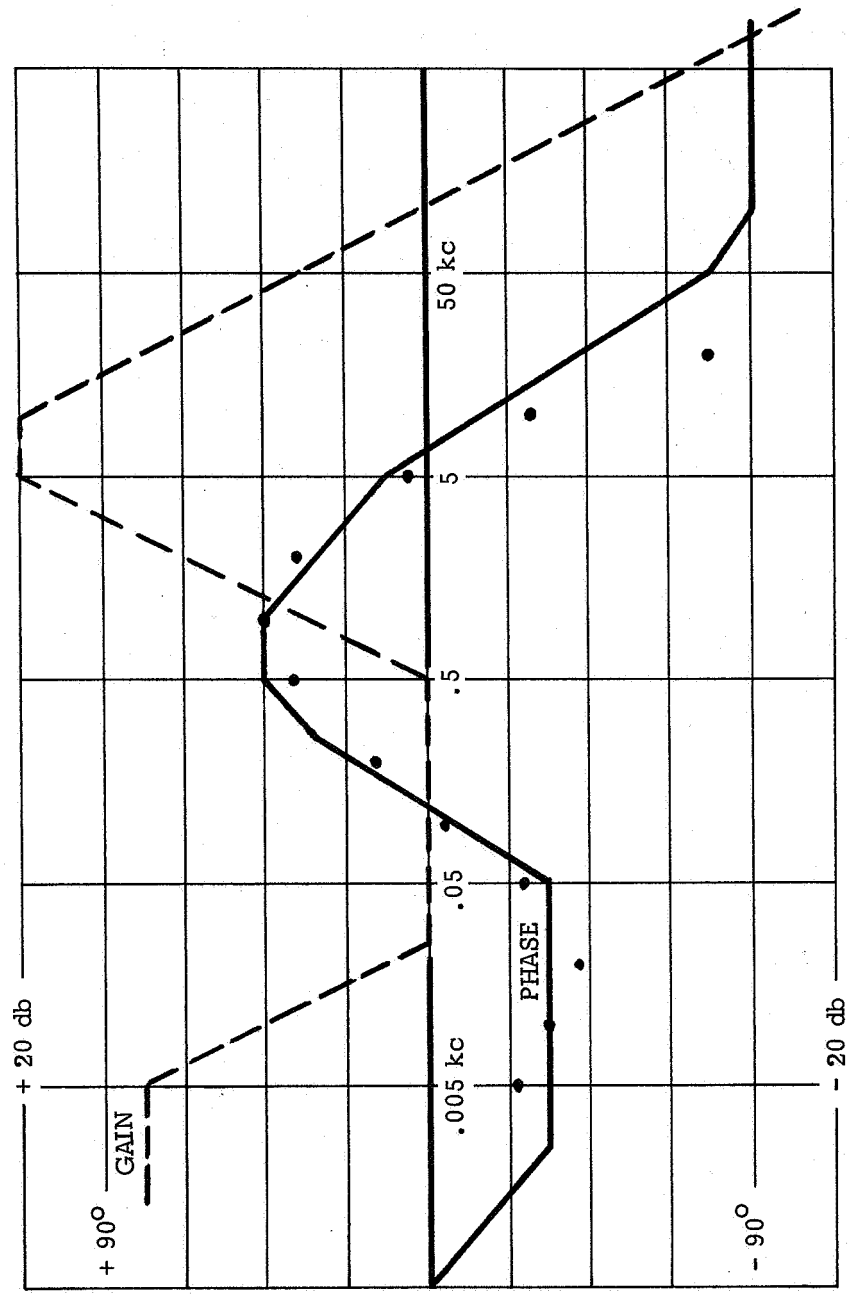

Design gain (—), design phase (—) and experimentally measured phase (•) of compensation amplifier as functions of frequency.

Figure 12 Suspension Gain and Phase Characteristics

The modulated carrier rotor position error signal is generated by summing, at the base of Q_{13}, the time derivative of the potential difference on the two opposing suspension electrodes (terminal 22), and the difference of currents into the two electrodes (I, terminal 24). The relative proportion of these two summands must be adjusted correctly for the combination to be a true measure of rotor displacement; this adjustment is made by varying the 200-pF variable capacitor C_4. The criterion for correct adjustment is discussed in Section V.

All of the circuit components of Figures 10 and 11 have now been discussed in terms of their signal processing functions except for certain small capacitors (50-100 pF) connected to the bases of several of the transistors. All such capacitors go to bases driven by transformer windings, and serve to suppress a high frequency (~10Mc) parasitic oscillation observed at times and attributed to the small, but not negligible, leakage reactance of the transformer windings.

SECTION V
CIRCUIT ADJUSTMENT AND TUNING

The oscillator is adjusted for frequency, 120^{o} phase separation, and amplitude equality in the three sections as follows: Each section is first operated separately as a single-phase oscillator, and tuned to a frequency slightly above 40 kc by adjusting the tank circuit capacitor, and to an amplitude just short of saturation by adjustment of the resistor across the tank.

The sections are then coupled together as a three-phase system (Figure 9), the B_1 voltage is set at an intermediate value such as 12 volts, the normal loading is presented to terminals 2, 4 .... 12 and 24, 26 ... 34, and the three trimmer capacitors are adjusted for exact frequency and exact 120^{o} phase separation. The sum of the trimmer capacitances determines the frequency, and the distribution of the total trimmer capacitance among the three tanks determines the phase separation. Finally, the oscillation levels of the three sections are evened out by adding shunt resistance to whatever section is operating at a higher level than another. The collector voltage swing is about 20 volts peak-to-peak for 12 volts of B_1 supply.

The circuit of Figure 11 requires only one type of adjustment, the tuning of the series resonant circuits by removing turns from the inductors L_1 and L_2. This tuning must be done with the high voltage windings connected to the gyro electrodes, or to exactly equivalent capacitance.

The circuit of Figure 10 requires a whole series of adjustments. The parallel resonant circuits in the push-pull amplifier loads are tuned to resonance at 40 kc by trimming of capacitors C_1 and C_{19} and the shunt impedance checked to see if it is high enough ($\geq$ 1K). The phase shift between driver signal (Q_5, Q_6) and output current (I, I_o) is minimized by trimming the .015 μF coupling capacitors C_2 and C_{18}. The sign of the suspension loop feedback is verified

by checking that the electrode current increases on that side where the gap increases. The equilibrium position of the rotor is centered by adjusting the 10K potentiometer to make φ (the phase of I relative to I_o) equal to 90^o when equal capacitances are presented to the two high voltage terminals. The 200-pF capacitor C_4 is adjusted to minimize the change in error signal when φ is varied.

When the adjustments delineated above have all been made, a gyro is suspended with the circuit. This is done at a rather low B_1 voltage, such as 10 volts, and the suspension loop is activated in two stages: First the B_2 voltage is switched on and immediately thereafter the emitter resistors of the Q_{13} stages are switched to B_1, enabling the suspension feedback loops. This switching procedure has been found to suspend the rotor reliably and with minimum arcing and minimum disturbance of the vacuum.

After rotor suspension, a final adjustment of the 200-pF capacitors C_4 is made while observing the response of the suspension loop to a step disturbance. The step disturbance is injected by connecting 100 to 300K between the Q_{12} collector and ground, and observing the envelope of the rotor displacement signal when the resistor is disconnected. Adjustment is made for the design resonant frequency of 400 cps at B_1 = 10 volts and for optimum damping.

SECTION VI
REFLECTED VOLTAGE PROBLEM

Early in 1966, a basic difficulty was uncovered in the circuit design approach for a low power, low torque suspension system. In brief, the power factor-correcting schemes which had been planned to achieve high amplifier efficiency, and correspondingly low power drain, were found to cause amplifier saturation when the rotor is displaced from center by more than about 10% of the gap. A satisfactory suspension system must be free of amplifier saturation phenomena for all geometrically possible rotor locations, because if ever an amplifier saturates, the servo loop of which that amplifier is a part is temporarily paralyzed and inoperative. The variability of the reactances between rotor and electrodes is the primary source of the difficulty.

The difficulty was overcome after an intensive search for methods of preserving both high efficiency and freedom from saturation in the amplifiers. The solution consists of adaptive control of the B_2 voltage applied to the output push-pull amplifiers, in such a way as to keep those amplifiers always just clear of saturation. When the rotor is centered within 10% of the gap, the B_2 voltage will be low and the efficiency high, but on those rare occasions when the rotor is displaced more than 10%, as during initial liftoff or during severe g-loading, the B_2 voltage will rise to prevent saturation and the efficiency will suffer. Thus, the long time average efficiency may be expected to be high. The solution is compatible with the phase modulation scheme which always has been central to the project because of its advantageous force-deflection characteristics and its natural preservation of the sum of forces requirement for minimizing torque.

Voltage-controlled variable reactors would also, in principle, permit operation at high amplifier efficiencies under all circumstances. However, based on previous experience with variable reactors, it was concluded that they cannot be made to respond rapidly enough without themselves using up as much power in the bias current circuits as they save in the main amplifiers.

Since amplifier efficiency and saturation problems are of basic importance in EVG suspension art, a more detailed technical discussion will be given below.

A practical effect of these developments has been to require a major change in the transformer turns ratio, plus the development of an adaptive control circuit which senses how near the amplifiers are to saturation and sets the B_2 voltage accordingly. The latter circuit has been breadboarded and tested successfully.

The problem can be discussed in terms of a single individual axis, i.e., one pair of diametrically opposite electrodes and the rotor:

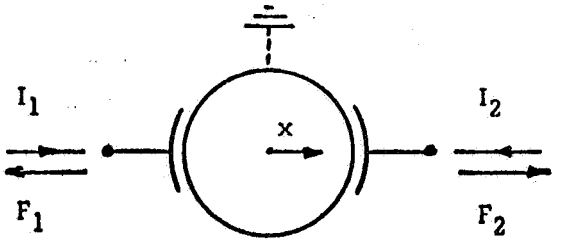

The influence of the other axes of the full suspension system can be described completely by the statement that the ac rotor potential is held at ground.

The function of the suspension electronics is to drive ac currents I_1 and I_2 into the two suspension electrodes, thus creating forces

$$F_1 = \frac{18\pi \times 10^{18} I_1^2}{\omega^2 A} \text{ dynes and } F_2 = \frac{18\pi \times 10^{18} I_2^2}{\omega^2 A} \text{ dynes}$$

where the currents are measured in amperes, ω is the radian frequency of the currents and A is the electrode area in cm^2. The net force is $F_2 - F_1$, proportional to $I_2^2 - I_1^2$, and the sum of forces is $F_2 + F_1$, proportional to $I_1^2 + I_2^2$. Since the gap capacitance varies inversely as the gap, the individual reactances depend on rotor displacement x as:

$$X_1 = -\frac{1}{\omega C_1} = -X_o\left(1+\frac{x}{d}\right) \qquad X_2 = -X_o\left(1-\frac{x}{d}\right)$$

The negative sign indicates that the reactance is capacitive; d is the nominal gap dimension.

Since the electrode voltages are generally too high for direct transistor drive, and since it is desired to couple one amplifier to the sum of the two currents and another to the difference, a transformer is connected to each of the electrode terminals and the following circuit is arrived at:

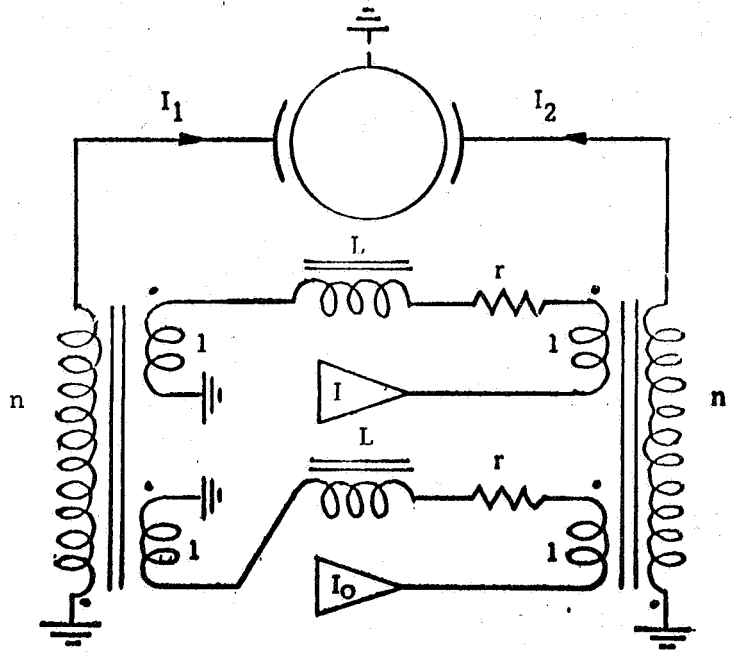

The two amplifiers have high output impedance ("constant current" generators). By straightforward application of Kirchhoff's laws it is found that the currents supplied by the two amplifiers are

$$I_o = \frac{n}{2}(I_1 + I_2) \qquad I = \frac{n}{2}(I_2 - I_1)$$

and the voltages at the amplifier terminals are

$$V_o = \left[j\left(\omega L - \frac{2X_o}{n^2}\right) + r\right] I_o + \frac{x}{d}\,\frac{2jX_o}{n^2}\, I$$

$$V = \left[j\omega L - \frac{2X_o}{n^2} + r\right] I + \frac{x}{d}\,\frac{2jX_o}{n^2}\, I_o$$

where n is the transformer turns ratio. The fixed reactors L, are chosen such that $\omega L = 2X_o/n^2$, i.e., to resonate the sum of the gap reactances, which is substantially a constant independent of rotor location. This means that if either amplifier alone were driving the circuit, it would be working into a small resistive load $r = \omega L/Q$, $Q \cong 10$ to 15, representing the losses in the coils and transformers, and could be designed to operate at high efficiency into that load. But as can be seen from the voltage formulae, there are two other terms proportional to x/d in the amplifier terminal voltages. These terms are referred to as "reflected voltages" because they are generated at a given amplifier terminal by reflection of the excitation from the other amplifier. The reflected voltages are very troublesome because they can be larger than rI_o, respectively, rI by a factor Q; they are not compensatable by constant reactances because they vary with x, and they tend to make the amplifier terminal voltage exceed the B_2 voltage and thus saturate the amplifier.

In the phase modulation scheme, the two currents, I_o and I, are kept at equal constant amplitude and only the phase of I is varied to control the net force $F_2 - F_1$, while keeping the sum of forces $F_1 + F_2$ constant. Thus, each amplifier will be subject to a reflected voltage of the same magnitude if x/d is appreciable.

The method developed for dealing with the reflected voltages is as follows: Select the turns ratio so that the maximum reflected voltage is just within the maximum voltage capability of the amplifier, which is determined by the maximum voltage rating of the transistor used; n = 20 is appropriate for the currently employed 2N2907 transistor; n = 10 would be appropriate for a high voltage transistor such as the 2N3497. As soon as n is fixed, the inductors L can be wound. A diode is connected to every push-pull amplifier collector in the system and all these diodes are "OR'd" together to detect the greatest voltage excursion of any collector.

The B_2 voltage on all the amplifiers is controlled by this signal to maintain the voltage at the least value consistent with unsaturated operation. Therefore,

when x/d is small (of order 1/Q or less), the high efficiency condition will be met by applying a low B_2 voltage; when x/d is large,the B_2 voltage will rise to prevent saturation. The transistors will be adequately heat-sinked and the momentary high dissipation in them when x/d is appreciable will be kept within the transistor rating.

The means for supplying variable voltage power efficiently have been discussed before in connection with the variation of the system excitation for g-adaptivity. Such means are well-known; the simplest form being a high frequency switch which connects a reactor alternately to a fixed high voltage and to the variable low voltage. The voltage is varied by changing the relative dwell time of the switch in the two positions. The dc-to-dc converter was not built because excellent regulating circuits of commercial power supplies were available to perform the function during the development program.

SECTION VII
CONCLUSIONS AND RECOMMENDATIONS

CONCLUSIONS

It seems clear that the development work and test results reported here have established the feasibility of a phase modulation suspension circuit for electrical vacuum gyro rotors and the practical realization of its several advantages. In addition to the advantages anticipated at the beginning of the project, namely reliable and efficient amplifier performance, g-adaptive capability, power saving, high stiffness at low frequencies, and automatic constancy of the sum of forces, other advantages have shown up in the course of operation: A gyro can be initially suspended at the throw of a switch with little or no voltage flash-over, minimizing damage to the rotor surface. The final adjustment of the circuit to match the exact capacitances of the gyro can be done with the rotor continuously suspended, because unlike the amplitude modulation circuit, this circuit engages in limited (small) amplitude oscillations when moderately mistuned. The tuneup procedure appears quite amenable to reduction to a routine operation by an unskilled person. These newly discovered advantages are attributed to the purposeful nonlinearity designed into the circuit, which is inherent in the phase modulation system and, in any case, necessary for sum of forces constancy.

The only one of the anticipated advantages of which there is no experimental confirmation in the tests to-date is the sum of forces constancy which is expected to reduce certain drift coefficients in the drift performance model. Unfortunately, the only gyro available for a drift test run at the time when the run had to be made was in very poor mechanical condition so that "pattern torques" were large enough to mask the sum of forces improvement. However, the theoretical basis for expecting an improvement in the sum of forces drift coefficient remains as sound as ever.

RECOMMENDATIONS

As a general recommendation, the phase modulation concept should be pursued further in order to perfect and refine it.

Several specific areas for improvement have suggested themselves in the course of the work:

1. Six-axis system instead of three. Several advantages of the six-axis system over the three-axis system are apparent, namely, redundancy of suspension axes, i.e., failure of one axis will not cause failure of the suspension system, cancellation of an additional (fourth order) drift coefficient, statistical averaging of sum of forces discrepancies, 15% more g capability for the same electrical excitation, less cross coupling between axes, smaller rotor displacement tolerances, and more nearly constant sum of gap reactances.

   An additional advantage of the six-axis configuration has appeared: In the six-axis system the total g load is shared in such a way that, at most, half the load is on any one axis and the neighboring five then each take 1/10 the load. This means that even when one axis is near its maximum load capability and its incremental stiffness is very low, the neighboring axes are individually lightly loaded and providing maximum incremental stiffness. The net result is that the stiffness and damping of a six-axis system will hold up much better than those of a three-axis system under heavy loading.

   Little new design effort is involved in the changeover to a six-axis system, and it amounts to little more than duplication of the parts of the circuit specific to particular axes. The three-phase oscillator would remain unchanged and each of its phases would drive two axes.

   In summary, changeover to a six-axis phase modulation system is recommended as being advantageous and straightforward.

2. Decrease of dc gain and offsetting increase in ac gain in the suspension feedback loop is recommended. The present circuit is not optimum in this respect since it has a dc voltage gain of about 13 and quite low level ac error signal (about 1.5 volts peak-to-peak for bottomed rotor), making it susceptable to electrical disturbances such as ac pickup and demodulator switch noise.

3. The adjustment of the 200-pF variable capacitor C_4 (Figure 10) is unduly critical and changes with gyro gap capacitance. It is recommended that a means be determined for reducing the sensitivity of this adjustment, or of eliminating the adjustment entirely.

4. In the present circuit, the gains vary with B_1 in such a way that the suspension resonant frequency varies approximately linearly with B_1, or as the square root of the maximum g capability. This condition makes it difficult to provide good damping over a wide range of g capabilities. It is recommended that means be determined for reducing the dynamic range of resonant frequencies for a given range of B_1 voltages.

5. In the present circuit, the power consumption (shown in Figure 4(b)) goes almost entirely to heating the transistors of the output push-pull stages; in other words, the output amplifier efficiency is still low, mainly because the transistors must be kept clear of saturation in the presence of the "reflected voltage". It is recommended that further effort be devoted to increasing amplifier efficiency.